THE JOURNAL OF PHYSICAL CHEMISTRY B

Article

Cite This: J. Phys. Chem. B 2019, 123, 1248−1255

pubs.acs.org/JPCB

Identification of Common Resonant Lines in the EPR Spectra of Melanins

João V. Paulin,*[,†] Augusto Batagin-Neto,[†,‡] and Carlos F. O. Graeff[†,§]

[†]São Paulo State University (UNESP), School of Sciences, Postgraduate Program in Materials Science and Technology (POSMAT), Bauru 17033-360, Brazil

[‡]São Paulo State University (UNESP), Campus of Itapeva, Itapeva 18409-010, Brazil

[§]São Paulo State University (UNESP), School of Sciences, Department of Physics, Bauru 17033-360, Brazil

Supporting Information

ABSTRACT: Melanins are natural pigments with promising bioelectronic applications. Among their unique properties, the existence of a persistent paramagnetic signal can be considered one of the most intriguing and controversial features. Additionally, the possible influence of such centers on charge transport accentuates the need for a better understanding of their origin and specific characteristics. In this report, electron paramagnetic resonance spectra of melanin samples obtained at different experimental conditions were systematically studied. From the fitting procedure, three distinct resonant lines are proposed, two associated with carbon-centered radicals and one with semiquinone free radicals.

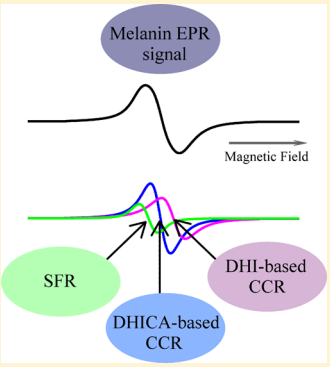

INTRODUCTION

Melanin is an important class of natural pigments that has multiple functions in the human body, such as photoprotection, antioxidant activity, and free-radical scavenging, and is thus associated with relevant health problems such as melanoma and neurological disorders.[1] In humans, melanin can be found in two forms that are distinguished by their coloration: black-brown eumelanin and red-yellow pheomelanin.[1,2] Among them, eumelanin (called herein as melanin) is the most abundant and also the most relevant from technological and biological points of view.

Melanin is an indolequinone-based bio-macromolecule mainly composed of 5,6-dihydroxyindole (DHI) and 5,6-dihydroxyindole-2-carboxylic acid (DHICA) monomeric structures in various redox forms (see Figure 1).[1,2] Melanin has become a material of technological relevance, especially in the field of bioelectronics, due to its unique physical and chemical properties, such as biocompatibility and biodegradability, metal chelation, broad absorbance throughout the UV−vis region, strong nonradioactive relaxation of photoexcited electronic states, and mixed ionic/electronic conductivities.[1−4] Since some of these physicochemical properties have been associated with the persistent and stable free radical in the melanin structure,[2,3,5−7] an in-depth understanding of its properties is fundamental.

To date, different experiments have shown that melanin presents at least two distinct paramagnetic centers that can be detectable in both solid-state and aqueous suspensions. These centers can be distinguished by their *g*-factors and line shapes.[7−12] It was proposed that the carbon-centered radicals (CCRs) are usually protected from the environment, being located in internal regions of the melanin structure. This center is found in acidic and neutral samples (dry powder or solutions/suspensions) and has a weak dependence on temperature and pH. On the other hand, the second paramagnetic species, known as semiquinone free radicals (SFRs), dominate the electron paramagnetic resonance (EPR) spectra of alkaline samples/solutions, presenting a strong dependence on pH (especially the signal intensity). Moreover, these paramagnetic species present similar *g*-factors, with 2.003 for CCR and 2.005 for SFR.[11,12]

In general, the concentrations of the semiquinone radicals in melanin solutions/suspensions are discussed in terms of the comproportionation equilibrium described by eq 1

$$Q + QH_2 + 2H_2O \rightleftharpoons 2H_3O^+ + 2SQ^* \quad (1)$$

where Q and QH_2 represent, respectively, quinone and hydroquinone species, while SQ* represents the semiquinone free radical. In alkaline solutions and hydration-dependent experiments, the reaction shifts toward the products and in acidic samples, toward the reactants, which changes the relative intensity of CCR and SFR components in the spectra.[2,11]

In fact, although there are a good number of studies on the paramagnetic properties of melanin, to date, there is no

Received: October 4, 2018
Revised: January 13, 2019
Published: January 17, 2019

DOI: 10.1021/acs.jpcb.8b09694
J. Phys. Chem. B 2019, 123, 1248−1255

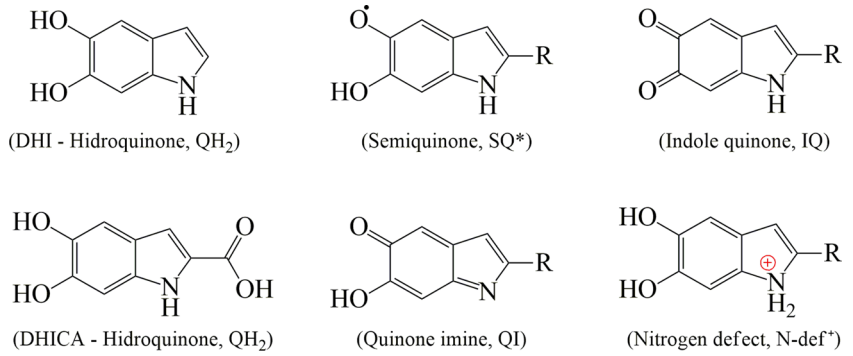

Figure 1. Different redox forms of melanin monomeric structures: R = H (DHI) or COOH (DHICA).

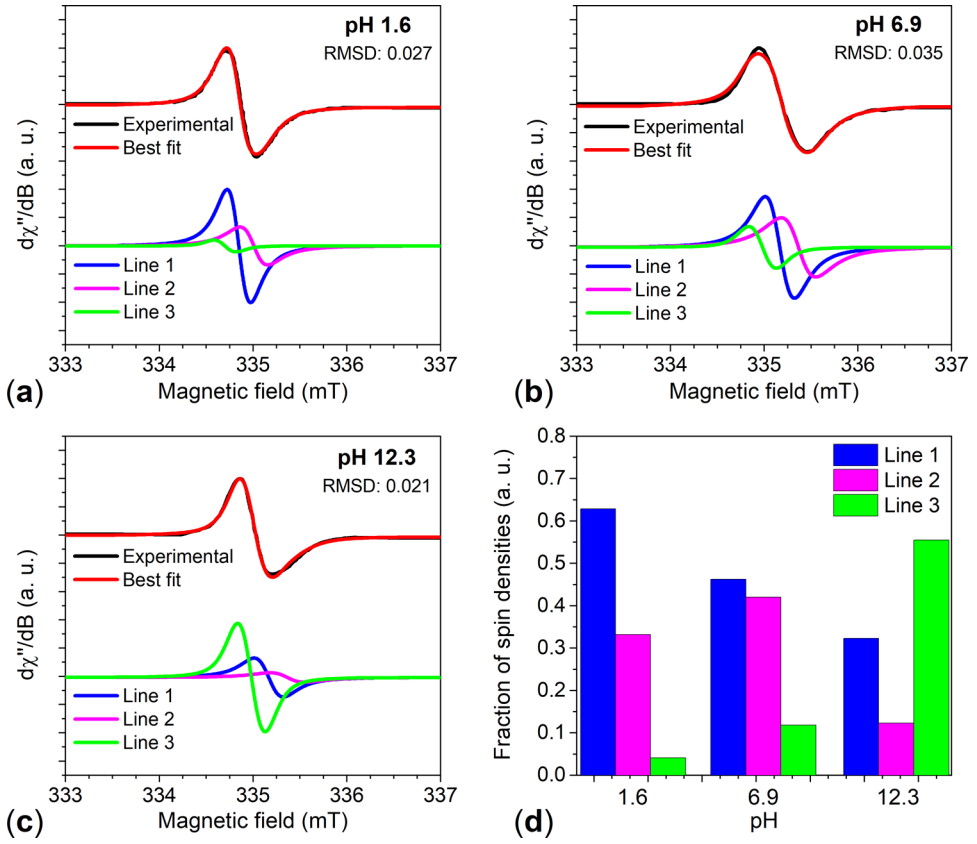

Figure 2. Melanin X-band EPR spectrum simulation at pH values (a) 1.6, (b) 6.9, and (c) 12.3. (d) Estimation of the spin densities of each component of the melanin EPR line for the different pH values. The black line represents the experimental spectra, while the red line represents the simulated ones. The blue, pink, and green lines and bars represent the three components used in the fit. Experimental data reprinted with permission from Chio et al.[10] Copyright 1982 Published by Elsevier Inc.

consensus on the nature of the paramagnetic species existing in these systems, especially regarding the CCR signals. In an attempt to correlate the melanin structures to the paramagnetic centers responsible for EPR spectra, DFT calculations of *g*-factors and hyperfine coupling constants were carried out by our group.[12] Monomeric and dimeric structures were evaluated from the most common EPR-active or paramagnetic (with one unpaired electron in the ground state) redox forms of melanin (Figure 1), i.e., positively and negatively charged species for structures with an even number of electrons (QH_2, IQ, QI, and N-def$^+$) and neutral for structures with odd number of electrons (SQ*).

In that study, it was shown that the signals generically described as SFR can be associated with fully oxidized and semioxidized monomers (IQ anion and SQ* radicals), while CCRs were assigned to negatively charged structures of hydroquinone (QH_2) and nitrogen-protonated defects (N-def$^+$). In particular, N-def$^+$ species can be considered as a subproduct of melanin synthesis,[13] whose existence has been observed in several melanin derivatives.[14−17]

In this study, we have carried out EPR spectra simulation from our data and the literature. The results indicate the existence of three components, which combined to form an asymmetric EPR signal. Comparative analyses considering distinct samples suggest that the CCR signals of DHI and DHICA species can be distinguished.

DOI: 10.1021/acs.jpcb.8b09694
J. Phys. Chem. B 2019, 123, 1248−1255

EXPERIMENTAL SECTION

Sample Preparation. Two melanin analogues with slightly different chemical structures were synthesized in water, following the literature.[16] Briefly, 0.3 g of 3,4-dihydroxy-DL-phenylalanine (DL-DOPA, Sigma-Aldrich) was dissolved in a mixture of 60 mL of Milli-Q water and 400 μL of ammonium hydroxide (28−30%, Synth) at room temperature (ca. 27 °C). The pH of the solution was always between 8 and 9, and it was kept under stirring and oxygenation using an air pump (HMel) for 3 days or for 6 h under 6 atm of O_2 pressure in a stainless steel reactor with a capacity of 150 mL (HMel-6P). For extraction and purification, both samples were immersed in Milli-Q water inside a dialysis membrane of 3500 molecular weight cut-off and then kept for 48 h in a stove at 80 °C for drying and just prior to measurements for 2 h to keep them dry.

All commercial chemicals were used without further purification.

X-Band EPR Measurements, Data Collection, and Spectra Simulations. EPR measurements of HMel and HMel-6P were performed in solid-state using an X-band spectrometer MiniScope MS300 (Magnettech). The microwave frequency was measured using an Agilent Frequency Counter 53181A RF. The microwave power ranged from 0.10 to 50.12 mW. For *g*-factor calibration, 2,2-diphenyl-1-picrylhydrazyl (DPPH, g = 2.0036) was used.

Some of the EPR spectra were extracted from the works of Chio et al.,[10] Mostert et al.,[11] and Panzella et al.[18] employing the software WebPlotDigitizer.[19] Spectra simulation was done using EasySpin (v. 4.5.5)[20] implemented in the Matlab software package, using Voigtian line shapes with isotropic broadening. Pepper and garlic routines were employed in the fitting procedure for powders and solutions, respectively.[20] OriginPro 9.0 computational package[21] was used for interpolation and spin concentration determination. To reduce the number of variables involved in the fittings and then turn it feasible, we have tried to keep as fixed as possible the parameters associated with signal line shapes and widths during the fittings.

RESULTS AND DISCUSSION

The EPR spectra of natural and synthetic melanin under different pH conditions reported by Chio et al.[10] were used as starting point. At first, only two resonant components were employed to fit the spectra, with no success. For most of the cases, a good fit was observed in the central region of the spectra with large deviations elsewhere. In particular, with only two components, it was not possible to adjust the typical asymmetries observed in the spectra (see Figure S1 in the Supporting Information for details). These difficulties were overcome by considering a third component.

Figure 2a−c illustrates the results obtained for the experimental data reported by Chio et al.[10] at distinct pH values (1.6, 6.9, and 12.3, respectively). The experimental, simulated, and individual signals of the three components are presented in black, red, and blue-pink-green lines, respectively. It is important to stress that despite employing three distinct resonant lines (RLs) to fit the spectra presented in Figure 2, the *g*-factors and line widths (ΔH_{pp}) were kept fixed for each component, and the only free parameter was the intensity of the components. As can be seen, a good adjustment is obtained (RMSD < 0.040), which suggests that at least three populations of distinct paramagnetic centers are present in these samples. The changes in intensity presented in Figure 2d are partially explained by the comproportionation reaction (eq 1). Note that components **1** and **3** follow strictly the trend imposed by eq 1, while component **2** has no clear dependence.

Table 1 shows the spectroscopic parameters estimated for each component of the simulated spectra.

Table 1. Spectral Parameters of the Simulated Signals

lines	*g*-factor	ΔH_{pp} (mT)	assignment
1	2.0038	0.380	CCR
2	2.0026	0.396	CCR
3	2.0049	0.350	SFR

In general, there is a consensus in the literature that CCR species dominate the EPR spectra of melanin suspensions at low pH, while SFR at higher pH, which is explained by changes induced by OH^- and/or H_2O species in the balance of eq 1. In Figure 2 and Table 1, notice that component **3** presents the highest *g*-factor and the lowest line width, compatible with SFR.[5,11,12] On the other hand, components **1** and **2** are dominant at low pH, which indicates that both refer to CCR.[2,11] Note that the ΔH_{pp} values of CCR and SFR components are similar, which suggests that the larger line widths typically ascribed to CCR species in the literature[10] could be linked to the superposition of two signals with slightly different *g*-factors.

As a matter of fact, the existence of more than two paramagnetic species in melanin has already been proposed using Q-band EPR;[22,23] however, the great challenge is understanding their origin. In a previous work of our group, we have demonstrated through DFT calculations that charged and radical species of melanin units (Figure 1) have different EPR signatures.[12] In particular, it was shown that signals with higher *g*-factors and relatively low line widths (i.e., smaller hyperfine constants) associated with SFR centers could be ascribed with IQ^- and SQ* species, compatible with the literature.[2,11,24] On the other hand, on the basis of the calculated *g*-factors, the CCR signals should be ascribed to several species, such as neutral N-def$^+$ (N-def), QH_2 anion, QH_2 cation, and QI cation; however, for the proposition that CCRs should present larger unsolved hyperfines, associated with the high ionization potentials of the structures, N-def and QH_2 anion were proposed as the most likely species. Nonetheless, the mechanism associated with the formation of such species into melanin macromolecule is not easy to understand, mainly QH_2 anion.

Indeed, as evidenced in Figure 3, the LUMO levels of the QH_2 are quite high compared to other subunits so that QH_2 are not supposed to act as electron traps in the melanins (see Supporting Information for details regarding the calculations involved). In this context, a relevant mechanism that was not considered in our previous work is the role of N-def$^+$ structures as electron acceptors into the melanin macrostructure. Such species could be considered as byproducts of the melanin synthesis, being already identified in several melanin samples.[13−17] From a naive analysis of Figure 3, it is possible to see that since N-def$^+$ is present in the macromolecular structure of melanins (protected from the environment), it acts as a strong electron acceptor, mainly from QH_2 species, leading to the formation of the paramagnetic species N-def (neutral)

DOI: 10.1021/acs.jpcb.8b09694
J. Phys. Chem. B 2019, 123, 1248−1255

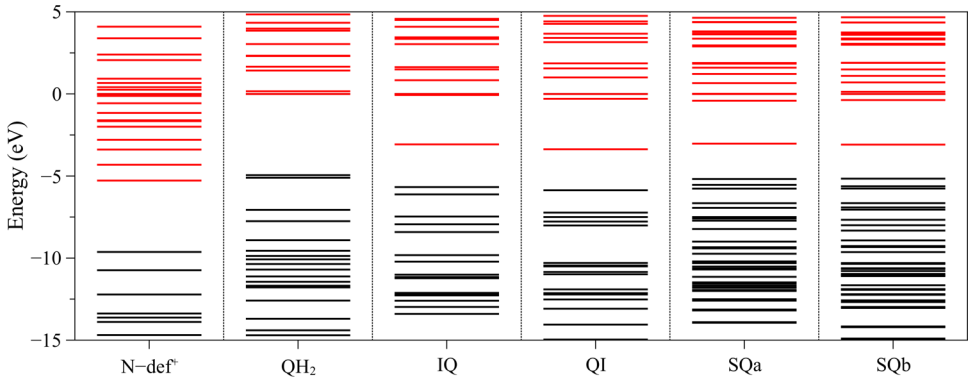

Figure 3. Energy levels around the frontier orbitals of melanin subunits. Colors represent occupation—black: occupied orbitals; red: unoccupied orbitals; and gray: semioccupied orbitals.

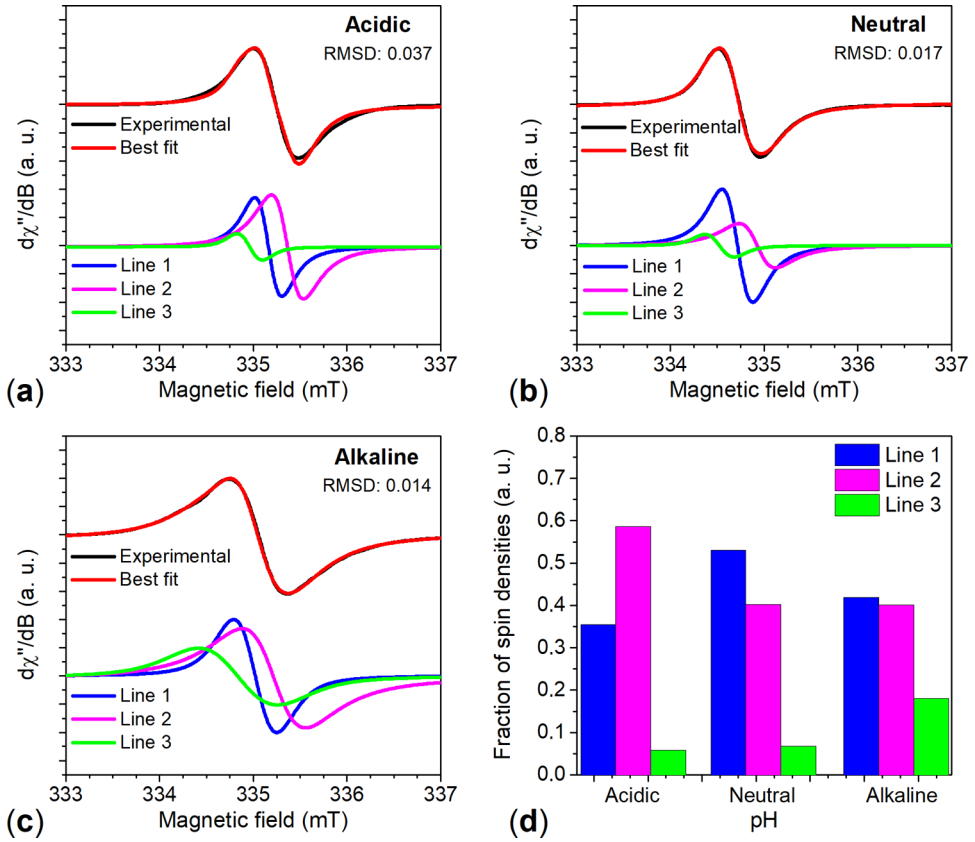

Figure 4. Melanin X-band EPR spectra simulation obtained from (a) acidic, (b) neutral, and (c) alkaline solid-state samples in hydration-controlled conditions. (d) Spin densities estimation for each component of the different samples. Experimental data reprinted with permission from Mostert et al.[11] Copyright 2013, American Chemical Society.

and QH_2 cation in the system, whose EPR parameters are compatible with the CCR signal.[12]

This result is consistent with the weak dependence of CCR spin densities on pH. Since the N-def$^+$ structures can be considered a kind of QH_2 species with a H^+ ion adsorbed on the nitrogen (that is trapped between the melanin layers), they are supposed to stabilize in the bulk of the macromolecule, protected from the changes in the environment. This result is also compatible with the destacking mechanism proposed by Mostert et al., which explains the weak consumption of CCR centers induced by melanin hydration that induces destacking of the melanin layers and exposure of such species.[11]

Another relevant feature from DFT is the prediction of higher *g*-factors and lower effective hyperfines for DHICA compared to DHI. This result suggests that signals **1** and **2** can be associated with DHICA and DHI species, respectively, and consequently that EPR could be used to qualitatively measure the DHICA/DHI ratio in melanin.

To reinforce our proposal of three components composing melanin EPR signal, we have considered another work found in the literature that used hydration-controlled measurements on acidic, neutral, and alkaline solid-state melanin samples. Mostert et al.[11] showed that the EPR signal is dominated by CCR species, presenting small contributions of SFRs in alkaline samples. Figure 4 presents the best fits obtained

DOI: 10.1021/acs.jpcb.8b09694
J. Phys. Chem. B 2019, 123, 1248−1255

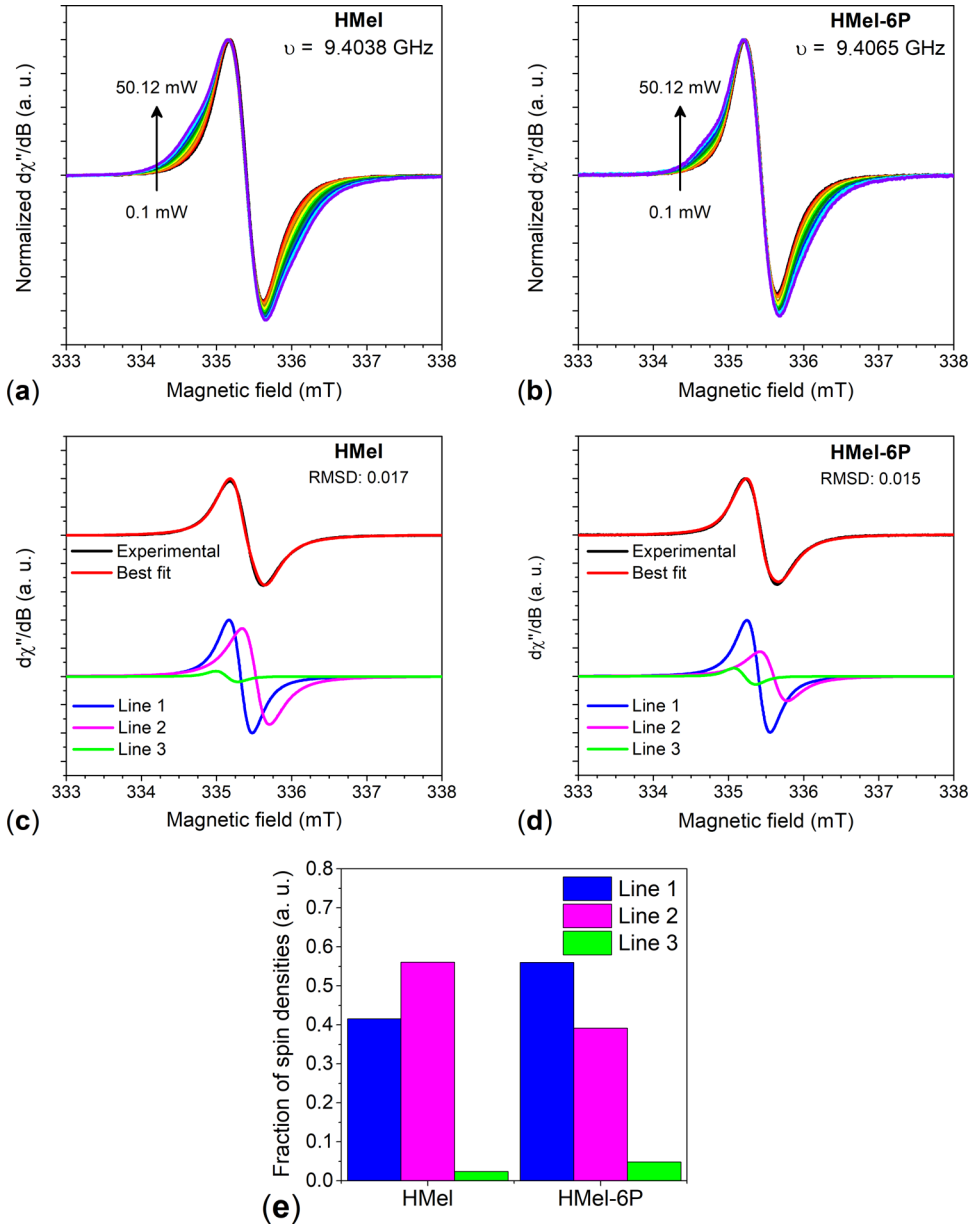

Figure 5. (a, b) X-band EPR spectra from 0.1 to 50.12 mW MWP and (c, d) EPR spectrum simulation obtained at 0.1 mW for (a, c) HMel and (b, d) HMel-6P. (e) Estimation of the spin densities of each component of HMel and HMel-6P for 0.1 mW of MWP.

from the experimental data considering three components. In these simulations, the spectroscopic parameters used are close to those in Figure 2.

As can be seen, good fits were obtained. As in Figure 2, three components are necessary to fit the spectra (see Figure S2 for fits based on two components). For the best fit, the same *g*-factor and line widths were used for acidic and neutral samples; however, for alkaline samples, although the *g*-factor remained the same, the line widths used were broader: 0.558, 0.672, and 1.000 for components **1**, **2**, and **3**, respectively. These deviations are assigned to the experimental procedure used to increase the sample pH, which may induce changes on the CCR species[5,11] and also induce degradation.

For solid samples, the spin densities of signals **1** and **2** are higher than the spin density of signal **3** independent of the pH, which was indeed expected, since a higher proportion of CCR species is commonly observed in solid-state samples. In particular, note that signals **1** and **2** have different dependencies on pH compared to solutions. In fact, Mostert and co-authors noted a decrease of the CCR signal intensity after alkalinization/hydration of the samples. Our results suggest that the CCR2 species (CCR associated with signal **2**) are initially more affected by hydration than the CCR1 ones (CCR associated with signal **1**). An opposite effect is observed for alkaline samples, leading to an equilibration between CCR1 and CCR2 populations.

Considering a possible association of CCR1 and CCR2 with DHICA and DHI paramagnetic species, such effects could be understandable based on the destacking mechanisms proposed by Mostert et al.[11] In this context, the water molecules could act as a destabilizing agent of the stacked substructures of melanin, facilitating the destacking and exposing the internal and previously protected CCR species to the environment. As a matter of fact, due to the typical connections between adjacent units,[2,11,18] this effect should be more pronounced in the DHI-based substructures than in the twisted DHICA,

DOI: 10.1021/acs.jpcb.8b09694
J. Phys. Chem. B 2019, 123, 1248−1255

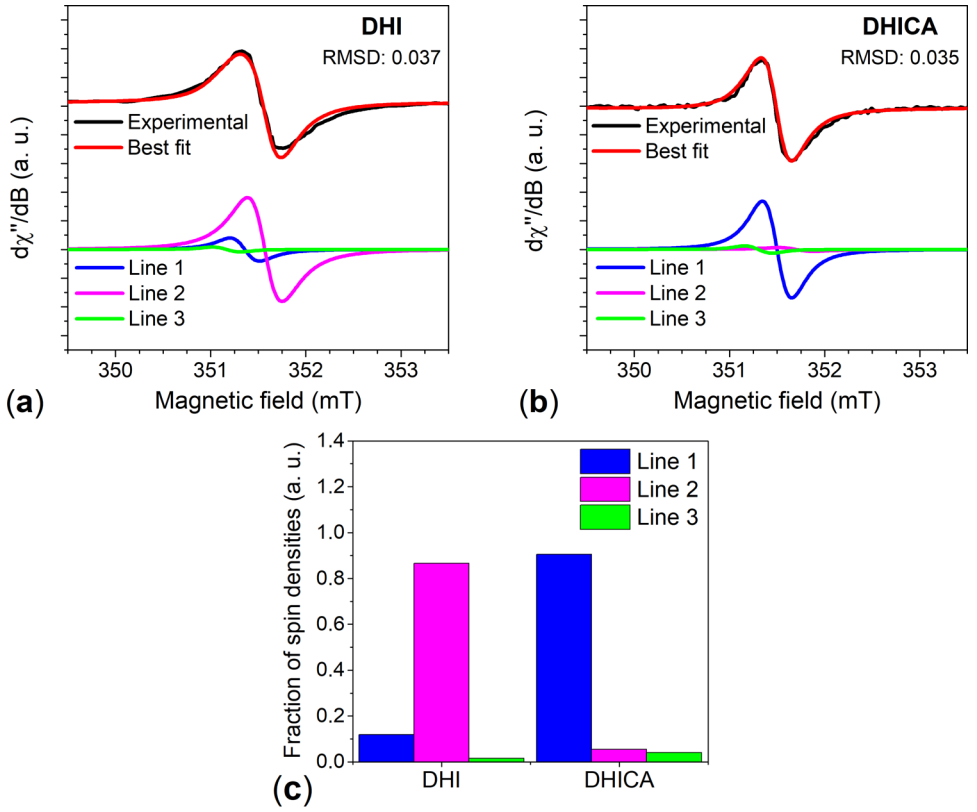

Figure 6. Melanin X-band EPR spectra simulation obtained from (a) DHI and (b) DHICA solid-state samples. (c) Estimation of the spin densities of each component of the EPR line for the different samples. Experimental data reprinted with permission from Panzella et al.[18] Copyright 2013 WILEY-VCH Verlag GmbH & Co. KGaA, Weinheim.

resulting in an apparent stabilization of CCR1 in wet samples. On the other hand, after the alkalinization of the samples, additional structural changes are observed as already identified in the parameters coming from the fittings, probably leading to the formation of additional centers or modified structures. Note that this result is in agreement with the previously discussed mechanism of CCR formation.

In addition, given the number of new routes that have been proposed to synthesize various melanin derivatives with slight differences in chemical structures, it is also interesting to evaluate if the same EPR components can still be employed for the fitting. Thus, we have carried out solid-state X-band EPR measurements on two distinct melanin samples: (i) non-carboxylate-rich structures (HMel), coming from traditional L-DOPA auto-oxidation with ammonium hydroxide and (ii) carboxylate-rich structures (HMel-6P), coming from a modified route recently proposed by our group.[16] Figure 5a,b shows the X-band EPR spectra obtained by varying the microwave power (MWP) from 0.1 to 50.12 mW for both samples.

At higher MWP, the EPR signal of both samples has a shoulder observable between 334 and 335 mT. This behavior is qualitatively similar to that reported by Mostert et al.,[5,11] suggesting that the signal at 0.1 mW is dominated by the CCR species that start to saturate at higher MWP.

When the simulation is performed in the spectra with the lowest MWP (0.1 mW), it is possible to observe a small contribution of the SFR species, while the CCR moieties dominate the spectra (see Figure 5c–e). Differently from the fittings of Figure 4c, the spectra presented in Figure 5c,d were simulated using the same spectral parameters employed in Figure 2 (*g*-factors and line widths). The most interesting is that the carboxylate-rich sample presents a higher intensity of CCR1 compared to the non-carboxylate-rich one (see Figure 5e).

It is important to mention that it is not adequate to fit the EPR signal at higher MWP (50.12 mW) mainly due to evident saturation of the spectra (see Figure S3). At this condition, the line shapes are distorted due to the saturation effect, hindering the identification of precise spectroscopic features due to dissimilar saturation regimes of the different components of the signal.[25,26]

To evaluate the plausibility of associating CCR1 and CCR2 with DHICA and DHI paramagnetic species, we simulated the solid-state EPR spectra of DHI- and DHICA-based melanin from the data reported by Panzella et al.[18] This is particularly relevant since the biological, structural, optical, and even paramagnetic/free-radical properties of melanins are generally governed by the proportion of DHICA over DHI structures.[1,2,18] In Panzella's work, DHI and DHICA melanin were obtained through L-DOPA oxidation by potassium hydrogen carbonate and potassium ferricyanide with sodium dithionite or sodium metabisulfite (for DHI or DHICA, respectively).[18,27] Figure 6 illustrates the three components-based fits for DHI and DHICA melanin (see Figure S4 for the simulations with only one or two components).

As can be seen in Figure 6, the EPR spectra are well fitted by three components, in which again CCR2 is assigned to DHI- and CCR1 to DHICA-rich samples. However, in this case, there is a clear predominance of one component, which reinforces our assignment.[27] In addition, note the low

DOI: 10.1021/acs.jpcb.8b09694
J. Phys. Chem. B 2019, 123, 1248–1255

contribution from SFR species (component **3**), in agreement with that proposed by Panzella et al.[18]

In summary, from the above-presented results, it is possible to identify the presence of three common paramagnetic species in distinct melanin samples. In particular, it is possible to associate two distinct species with the widely reported CCR centers, which can be assigned to DHI and DHICA paramagnetic moieties. The presence of these centers is responsible for the typical asymmetric line shape obtained from melanin. On the basis of the *g*-factors and line widths of the signals and energy-level alignments of the melanin units, it was possible to associate the CCR signals with QH_2 cation and N-def species.

CONCLUSIONS

In this report, we identify and discuss the nature of paramagnetic species found in different melanin samples. Our results suggest that the EPR spectra of melanin are generically composed of three distinct components, two of them being related to carbon-centered radical (CCR) species and the other to semiquinone free radicals (SFR).

Analysis of the ESR parameters and energy-level alignments of melanin subunits suggests that the CCR formation is associated with the presence of N-def^{+} species into the bulk of melanin macrostructure. The results coming from samples with distinct DHI/DHICA ratios suggest that the CCR components can be associated with DHICA and DHI species.

ASSOCIATED CONTENT

Supporting Information

The Supporting Information is available free of charge on the ACS Publications website at DOI: 10.1021/acs.jpcb.8b09694.

Additional EPR spectra simulations employing one and two paramagnetic species; normalized amplitude as a function of the power intensity; and electronic structure calculations (PDF)

AUTHOR INFORMATION

Corresponding Author

*E-mail: jv.paulin@unesp.br.

ORCID

João V. Paulin: 0000-0002-2379-6203

Augusto Batagin-Neto: 0000-0003-4609-9002

Notes

The authors declare no competing financial interest.

ACKNOWLEDGMENTS

The authors thank Dr. Marcus V. G. Vismara for assistance in EPR measurements. They acknowledge FAPESP (grant numbers 2012/03116-7, 2013/07296-2, and 2015/23000-1), CNPq (573636/2008-7), and CAPES for financial support.

REFERENCES

(1) d'Ischia, M.; Wakamatsu, K.; Cicoira, F.; Di Mauro, E.; Garcia-Borron, J. C.; Commo, S.; Galván, I.; Ghanem, G.; Kenzo, K.; Meredith, P.; et al. Melanins and Melanogenesis: From Pigment Cells to Human Health and Technological Applications. *Pigm. Cell Melanoma Res.* **2015**, *28*, 520−544.

(2) Meredith, P.; Sarna, T. The Physical and Chemical Properties of Eumelanin. *Pigm. Cell Res.* **2006**, *19*, 572−594.

(3) Mostert, A. B.; Powell, B. J.; Pratt, F. L.; Hanson, G. R.; Sarna, T.; Gentle, I. R.; Meredith, P. Role of Semiconductivity and Ion Transport in the Electrical Conduction of Melanin. *Proc. Natl. Acad. Sci.* **2012**, *109*, 8943−8947.

(4) Wünsche, J.; Cicoira, F.; Graeff, C. F. O.; Santato, C. Eumelanin Thin Films: Solution-Processing, Growth, and Charge Transport Properties. *J. Mater. Chem. B* **2013**, *1*, 3836.

(5) Mostert, A. B.; Rienecker, S. B.; Noble, C.; Hanson, G. R.; Meredith, P. The Photoreactive Free Radical in Eumelanin. *Sci. Adv.* **2018**, *4*, No. eaaq1293.

(6) Felix, C. C.; Hyde, J. S.; Sarna, T.; Sealy, R. C. Melanin Photoreactions in Aerated Media: Electron Spin Resonance Evidence for Production of Superoxide and Hydrogen Peroxide. *Biochem. Biophys. Res. Commun.* **1978**, *84*, 335−341.

(7) Felix, C. C.; Hyde, J. S.; Sarna, T.; Sealy, R. C. Interactions of Melanin with Metal Ions. Electron Spin Resonance Evidence for Chelate Complexes of Metal Ions with Free Radicals. *J. Am. Chem. Soc.* **1978**, *100*, 3922−3926.

(8) Blois, M. S.; Zahlan, A. B.; Maling, J. E. Electron spin resonance studies on melanin. *Biophys. J.* **1964**, *4*, 471−490.

(9) Chio, S.-S.; Hyde, J. S.; Sealy, R. C. Temperature-Dependent Paramagnetism in Melanin Polymers. *Arch. Biochem. Biophys.* **1980**, *199*, 133−139.

(10) Chio, S.-S.; Hyde, J. S.; Sealy, R. C. Paramagnetism in Melanins: pH Dependence. *Arch. Biochem. Biophys.* **1982**, *215*, 100−106.

(11) Mostert, A. B.; Hanson, G. R.; Sarna, T.; Gentle, I. R.; Powell, B. J.; Meredith, P. Hydration-Controlled X-Band EPR Spectroscopy: A Tool for Unravelling the Complexities of the Solid-State Free Radical in Eumelanin. *J. Phys. Chem. B* **2013**, *117*, 4965−4972.

(12) Batagin-Neto, A.; Bronze-Uhle, E. S.; de Oliveira Graeff, C. F. Electronic Structure Calculations of ESR Parameters of Melanin Units. *Phys. Chem. Chem. Phys.* **2015**, *17*, 7264−7274.

(13) Cánovas, F. G.; García-Carmona, F.; Sánchez, J. V.; Pastor, J. L.; Teruel, J. A. The Role of PH in the Melanin Biosynthesis Pathway. *J. Biol. Chem.* **1982**, *257*, 8738−8744 PMID: 6807981. .

(14) Clark, M. B.; Gardella, J. A.; Schultz, T. M.; Patil, D. G.; Salvati, L. Solid-State Analysis of Eumelanin Biopolymers by Electron Spectroscopy for Chemical Analysis. *Anal. Chem.* **1990**, *62*, 949−956.

(15) Bernsmann, F.; Ponche, A.; Ringwald, C.; Hemmerlé, J.; Raya, J.; Bechinger, B.; Voegel, J.-C.; Schaaf, P.; Ball, V. Characterization of Dopamine−Melanin Growth on Silicon Oxide. *J. Phys. Chem. C* **2009**, *113*, 8234−8242.

(16) Bronze-Uhle, E. S.; Paulin, J. V.; Piacenti-Silva, M.; Battocchio, C.; Rocco, M. L. M.; Graeff, C. F. deO. Melanin Synthesis under Oxygen Pressure: Melanin Synthesis under Oxygen Pressure. *Polym. Int.* **2016**, *65*, 1339−1346.

(17) Paulin, J. V.; Veiga, A. G.; Garcia-Basabe, Y.; Rocco, M. L. M.; Graeff, C. F. Structural and Optical Properties of Soluble Melanin Analogues with Enhanced Photoluminescence Quantum Efficiency: Melanin Analogues with Enhanced Photoluminescence Quantum Efficiency. *Polym. Int.* **2018**, *67*, 550−556.

(18) Panzella, L.; Gentile, G.; D'Errico, G.; Della Vecchia, N. F.; Errico, M. E.; Napolitano, A.; Carfagna, C.; d'Ischia, M. Atypical Structural and π-Electron Features of a Melanin Polymer That Lead to Superior Free-Radical-Scavenging Properties. *Angew. Chem., Int. Ed.* **2013**, *52*, 12684−12687.

(19) Rohatgi, A. *WebPlotDigitizer*; Austin, Texas, 2018.

(20) Stoll, S.; Schweiger, A. EasySpin, a Comprehensive Software Package for Spectral Simulation and Analysis in EPR. *J. Magn. Reson.* **2006**, *178*, 42−55.

(21) OriginLab Corp. *OriginPro*; MA.

(22) Grady, F. J.; Borg, D. C. Electron Paramagnetic Resonance Studies on Melanins. I. The Effect of PH on Spectra at Q Band. *J. Am. Chem. Soc.* **1968**, *90*, 2949−2952.

(23) Pasenkiewicz-Gierula, M.; Sealy, R. C. Analysis of the ESR Spectrum of Synthetic Dopa Melanin. *Biochim. Biophys. Acta* **1986**, *884*, 510−516.

(24) Sealy, R. C.; Hyde, J. S.; Felix, C. C.; Menon, I. A.; Prota, G.; Swartz, H. M.; Persad, S.; Haberman, H. F. Novel Free Radicals in Synthetic and Natural Pheomelanins: Distinction between Dopa

Melanins and Cysteinyldopa Melanins by ESR Spectroscopy. *Proc. Natl. Acad. Sci. USA* **1982**, *79*, 2885−2889.
(25) Poole, C. P. *Electron Spin Resonance: A Comprehensive Treatise on Experimental Techniques*; John Wiley & Sons: New York, 1983.
(26) Weil, J. A.; Bolton, J. R. *Electron Paramagnetic Resonance: Elementary Theory and Practical Applications*, 2nd ed.; Wiley: New York, 2006.
(27) Edge, R.; d'Ischia, M.; Land, E. J.; Napolitano, A.; Navaratnam, S.; Panzella, L.; Pezzella, A.; Ramsden, C. A.; Riley, P. A. Dopaquinone Redox Exchange with Dihydroxyindole and Dihydroxyindole Carboxylic Acid. *Pigm. Cell Res.* **2006**, *19*, 443−450.

DOI: 10.1021/acs.jpcb.8b09694
J. Phys. Chem. B 2019, 123, 1248−1255